

Controllable phase-dependent optical switch in an atom-cavity system

Xu-Yang Li(李旭阳), Yuan-Feng Lu(陆元峰), Ya-Jie Wu(吴亚杰), Ning Li(荔宁), and Miao-Di Guo(郭苗迪)
Citation: Chin. Phys. B, 2026, 35 (**2**): 024205. DOI: 10.1088/1674-1056/adfc40
http://cpb.iphy.ac.cn; http://iopscience.iop.org/cpb

What follows is a list of articles you may be interested in

Strain modulation of second harmonic generation in new tetrahedral transition metal dichalcogenide monolayers

Hu Chen(陈虎), Shi-Qi Li(李仕琪), Yuqing Wu(吴雨晴), Xiaozhendong Bao(鲍晓振东), Zhijie Lei(雷志杰), Hongsheng Liu(柳洪盛), Yuee Xie(谢月娥), Junfeng Gao(高峻峰), Yuanping Chen(陈元平), and Xiaohong Yan(颜晓红)
Chin. Phys. B, 2025, 34 (**8**): 084206. DOI: 10.1088/1674-1056/addaa3

Electromagnetically induced transparency via localized surface plasmon mode-assisted hybrid cavity QED

Xiaomiao Li(李晓苗), Famin Liu(刘发民), Zigeng Li(李子更), Hongyan Zhu(朱虹燕), Fan Wang(王帆), and Xiaolan Zhong(钟晓岚)
Chin. Phys. B, 2023, 32 (**11**): 114205. DOI: 10.1088/1674-1056/acd7d2

Absorption interferometer of two-sided cavity

Miao-Di Guo(郭苗迪) and Hong-Mei Li(李红梅)
Chin. Phys. B, 2021, 30 (**5**): 054202. DOI: 10.1088/1674-1056/abdea4

Polarization manipulation of bright-dark vector bisolitons

Yan Zhou(周延), Xiaoyan Lin(林晓艳), Meisong Liao(廖梅松), Guoying Zhao(赵国营), and Yongzheng Fang(房永征)
Chin. Phys. B, 2021, 30 (**3**): 034208. DOI: 10.1088/1674-1056/abd76d

Nonlinear coherent perfect photon absorber in asymmetrical atom-nanowires coupling system

Xiuwen Xia(夏秀文), Xinqin Zhang(张新琴), Jingping Xu(许静平), Mutian Cheng(程木田), Yaping Yang(羊亚平)
Chin. Phys. B, 2018, 27 (**11**): 114205. DOI: 10.1088/1674-1056/27/11/114205

Controllable phase-dependent optical switch in an atom-cavity system

Xu-Yang Li(李旭阳), Yuan-Feng Lu(陆元峰), Ya-Jie Wu(吴亚杰), Ning Li(荔宁), and Miao-Di Guo(郭苗迪)†

School of Sciences, Xi'an Technological University, Xi'an 710021, *China*

(Received 5 June 2025; revised manuscript received 31 July 2025; accepted manuscript online 18 August 2025)

Coherent perfect absorption (CPA) and coherent perfect transmission (CPT) are two extreme states arising from the manipulation of optical fields. Generally, CPA and CPT occur under different input-field phases. Therefore, we propose a scheme to realize an all-optical switch based on phase-dependent CPA–CPT conversion. In our proposal, the CPT state and the CPA state are treated as the on state and the off state, respectively. Consequently, the efficiency of this all-optical switch can reach the maximum value of 1. With the introduction of an incoherent pump field, the CPA state can be achieved under a weaker input probe field or can be converted into a CPT state. The results show that the optical switch can operate with weaker fields and can be further optimized by the application of an incoherent field.

Keywords: coherent perfect absorption, cavity-QED, optical switching

PACS: 42.50.–p, 42.50.Pq, 42.65.Pc

DOI: 10.1088/1674-1056/adfc40 **CSTR:** 32038.14.CPB.adfc40

1. Introduction

In recent years, the rapid advancement of quantum information networks and optical communication has brought the study of photon–photon interactions in quantum optics and quantum information processing to the forefront of scientific research. This progress has led to a growing interest in all-optical switches,[1–3] which utilize light to control light and offer significant advantages over traditional electro-optical switches in terms of response speed, signal loss, and device miniaturization.[4] Conventional all-optical switches typically rely on strong interactions between the control light and a coupling medium. However, such interactions often result in photon loss, thereby limiting switching efficiency. To address this limitation, various innovative approaches have been explored. For instance, multiple schemes have been proposed to design optical switches by employing diverse mechanisms, including near-field dipole–dipole interactions (NDD), ultrashort pulses in high-density media, and optical soliton interactions in birefringent fibers.[5–7] In recent years, interaction-free all-optical switches have been proposed to eliminate direct coupling between light beams, thereby suppressing signal photon loss in absorbing media and improving switching efficiency.[8,9] Additionally, bidirectional multi-channel all-optical switches have been demonstrated in electromagnetically induced transparency (EIT) media, offering high efficiency and wide bandwidth.[10] Nonlinear all-optical switches leveraging the negative dispersion properties of white-light cavities have also been introduced, reducing switching power without sacrificing speed.[11] Furthermore, the use of polaritons in Bose–Einstein condensates (BECs) has enabled high-speed switching at room temperature, contributing to advances in low-threshold lasers and quantum simulations.[12] Another promising approach involves exciton–polaritons in metal halide perovskites, where double-threshold behavior is exploited for efficient switching.[13] Additionally, some studies have investigated the influence of relevant parameters in three-soliton solutions on inelastic soliton interactions, providing an alternative route toward all-optical switching.[14] Despite these advances, the theoretical switching efficiency of all-optical switches has yet to reach 100%.

Coherent perfect absorption (CPA) offers a promising alternative for achieving high-efficiency all-optical switching. First proposed by Chong *et al.*[15] in 2010, CPA is a phenomenon that represents the time-reversed counterpart of laser emission. It has been demonstrated that manipulating the relative phase of incident lasers in silicon wafers can significantly modify photon absorption, enabling controllable CPA.[16] Moreover, studies have shown that tuning optical loss near exceptional points (EPs) allows the observation of CPA, where PT-breaking induces drastic changes in absorption.[17,18] With the rise of interdisciplinary research, CPA has been implemented in diverse systems, including metamaterials,[19] metasurfaces,[20] and graphene.[21] This unique mechanism has opened new possibilities for applications in optical modulation,[22] photodetection,[23] and optical sensing devices.[24] Owing to their low energy loss and controllable interaction strength, cavity quantum electrodynamics (QED) systems have been widely employed in all-optical switches and logic gates.[25] In such systems, CPA occurs when the phases of probe fields are matched across the cavity mirrors, leading to complete photon absorption under specific conditions. In contrast, phase mismatch prevents CPA and re-

†Corresponding author. E-mail: guomiaodi@xatu.edu.cn

© 2026 Chinese Physical Society and IOP Publishing Ltd. All rights, including for text and data mining, AI training, and similar technologies, are reserved.

sults in perfect photon output. Recent studies have demonstrated that tunable and switchable CPA can be realized using an incoherent field, further enhancing the performance of all-optical switches in cavity QED systems.[26]

In this study, we propose a phase-modulated all-optical switch in a two-level atom–cavity system controlled by an incoherent field. This scheme enables manipulation of the output intensity between CPA and coherent perfect transmission (CPT) states. In contrast to approaches based on non-Hermitian physics, our model adopts a Hermitian Hamiltonian to describe the total system energy. To account for open-system dynamics, dissipation is phenomenologically incorporated into the subsequent evolution equations. This treatment shares conceptual similarities with recent developments in non-Hermitian optics and photonics, particularly studies of PT symmetry and exceptional points. Although resonance phenomena have been extensively investigated and could, in principle, be rigorously analyzed using a quantum master equation, CPA has also been successfully demonstrated within PT-symmetric systems.[27] Unlike EIT-based switches, the proposed phase-dependent switch achieves 100% switching efficiency under optimal conditions. Our approach is grounded in semiclassical theory, in which the influence of the incoherent pumping field is introduced phenomenologically through its pumping rate. Although we are currently exploring CPA in a fully quantized multi-atom — single-mode field interaction model, the present work focuses on the semiclassical regime and does not address the complete quantum dynamics of the system. Nevertheless, the semiclassical framework provides experimentally testable predictions that can guide photonic device design. Specifically, our study not only enriches strategies for realizing highly efficient all-optical switches but also opens new possibilities for optical detection under weak-signal conditions. This paper is organized as follows. In Section 2, we present and analyze the atom–cavity coupling model. The numerical results are discussed in Section 3. Finally, Section 4 summarizes the work and outlines potential applications.

2. Theoretical model

The model diagram investigated in this work is shown in Fig. 1. The system consists of a single-mode cavity with volume V containing N cold two-level atoms. Two coherent lasers, denoted as $a_{\mathrm{in,l}}$ and $a_{\mathrm{in,r}}$, with frequency ω_{p} serve as probe fields and are injected into the cavity along the cavity axis. These fields drive the cavity mode from opposite directions with a frequency detuning $\Delta_{\mathrm{p}} = \omega_{\mathrm{p}} - \omega_{21}$.[28,29] The cavity mode with frequency ω_{c} couples to the atomic transition $|1\rangle \to |2\rangle$ with detuning $\Delta_{\mathrm{ac}} = \omega_{\mathrm{c}} - \omega_{21}$, where ω_{21} denotes the transition frequency between the ground state $|1\rangle$ and the excited state $|2\rangle$. Meanwhile, an incoherent field pumps the atomic population from $|1\rangle$ to $|2\rangle$. In the experiment, ^{85}Rb cold atoms ($N \sim 3\times10^5$) with $|1\rangle \equiv (5S_{1/2})$ and $|2\rangle \equiv (5P_{1/2})$ can be trapped at the center of a 5 cm cavity using a ^{87}Rb D_2-line (780 nm) magneto-optical trap. A millimeter-scale dual-port Fabry–Perot cavity with a finesse of $5.8(1)\times10^7$ is employed and operated at 1 K.[30] To probe the cavity response, a coherent 795 nm laser with tunable optical power serves as the probe field.[31] Precise control of the incident light intensity is achieved using a Mach–Zehnder interferometer,[32] which simultaneously compensates for relative phase drift induced by environmental disturbances.

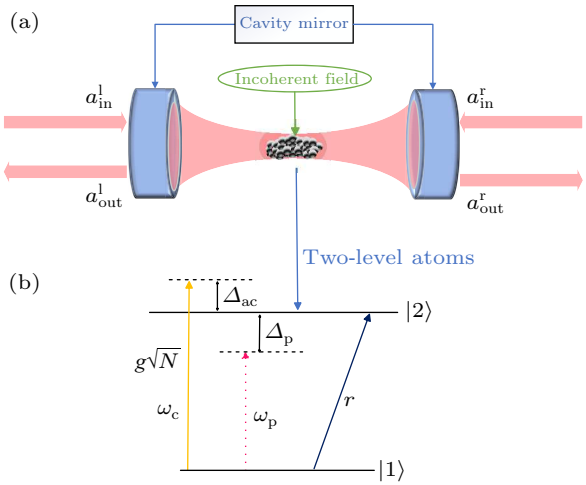


Fig. 1. (a) Schematic diagram of a cavity QED system consisting of a single-mode cavity driven by two coherent probe fields. (b) Energy-level diagram of two-level atoms inside the cavity.

In the rotating frame of the probe-field frequency, the system Hamiltonian (H) is derived under the rotating-wave approximation (RWA)

$$\Delta_{\mathrm{p}} = \omega_{\mathrm{p}} - \omega_{21} \ll \omega_{\mathrm{p}} + \omega_{21}, \tag{1}$$

$$\Delta_{\mathrm{ac}} = \omega_{\mathrm{c}} - \omega_{21} \ll \omega_{\mathrm{c}} + \omega_{21} \tag{2}$$

of the Jaynes–Cummings (JC) model as

$$H = \hbar\left[(\Delta_{\mathrm{ac}} - \Delta_{\mathrm{p}})a^{\dagger}a - \sum_{j=1}^{N}(\Delta_{\mathrm{p}}\sigma_{22}^{j} + ga^{\dagger}\sigma_{12}^{j} + ga\sigma_{21}^{j})\right]. \tag{3}$$

Here, $\hbar$ is the reduced Planck constant, $a^{\dagger}$ (a) represents the creation (annihilation) operator of the intracavity photon, and $\sigma_{mn}^{j} = |m\rangle\langle n|$ $(m,n = 1,2)$ denotes the atomic transition operator. The symbol N denotes the number of atoms inside the cavity, and $g = \mu_{12}\sqrt{\omega_{\mathrm{c}}/(2\hbar\varepsilon_0 V)}$ is the atom–cavity coupling coefficient. The electric dipole matrix element is μ_{mn}, ε_0 is the dielectric constant of free space, and V is the cavity mode volume.

The time evolution of the cavity QED system is governed by the Heisenberg equation of motion

$$\frac{\mathrm{d}\sigma}{\mathrm{d}t} = \frac{\mathrm{i}}{\hbar}[H,\sigma] + \mathcal{L}\sigma. \tag{4}$$

Here, the Lindblad superoperator $\mathcal{L}\sigma$ incorporates both cavity loss and atomic dissipation. Taking the collapse operator as

$\hat{C} = |g\rangle\langle e|$, we have[29,33]

$$\mathcal{L}_c\sigma = K\left(a\sigma a^\dagger - \frac{1}{2}\{a^\dagger a, \sigma\}\right), \tag{5}$$

$$\mathcal{L}_a\sigma = \Gamma\left(\hat{C}\sigma\hat{C}^\dagger - \frac{1}{2}\{\hat{C}^\dagger\hat{C}, \sigma\}\right). \tag{6}$$

The decay rate of the single-sided cavity mode is denoted by K, and the atomic decay rate by Γ.

To simplify the model, we adopt a mean-field approximation that neglects quantum fluctuation effects. This approximation ignores both the intrinsic quantum uncertainties of the system and the associated transient energy and particle fluctuations in the vacuum. By replacing the photon number operator $a^\dagger a$ with its expectation value $\langle a^\dagger a\rangle$, photon number fluctuations and the uncertainty relation between phase and particle number are effectively neglected. The resulting equations of motion read

$$\dot{\sigma}_{11} = \mathrm{i}g(a\sigma_{21} - a^\dagger\sigma_{12}) + \Gamma\sigma_{22} - r\sigma_{11}, \tag{7}$$

$$\dot{\sigma}_{12} = \mathrm{i}ga(\sigma_{22} - \sigma_{11}) - \mathrm{i}\Delta_p\sigma_{12} - \frac{\Gamma}{2}\sigma_{12}, \tag{8}$$

$$\dot{\sigma}_{22} = \mathrm{i}g(a^\dagger\sigma_{12} - a\sigma_{21}) - \Gamma\sigma_{22} + r\sigma_{11}, \tag{9}$$

$$\dot{\sigma}_{21} = \mathrm{i}ga^\dagger(\sigma_{11} - \sigma_{22}) + \mathrm{i}\Delta_p\sigma_{21} - \frac{\Gamma}{2}\sigma_{21}, \tag{10}$$

$$\dot{a} = \left[\mathrm{i}(\Delta_p - \Delta_{ac}) - \frac{\kappa_l + \kappa_r}{2}\right]a + \mathrm{i}gN\sigma_{12} + \sqrt{\kappa_l/\tau}a_{in}^l + \sqrt{\kappa_r/\tau}a_{in}^r. \tag{11}$$

Here, Γ is the relaxation rate of the excited state $|2\rangle$, r is the pumping rate of the incoherent field, κ_l (κ_r) denotes the field attenuation rate from the left (right) cavity mirror, and τ is the photon round-trip time in the cavity.

Assuming symmetric cavity mirrors ($\kappa_l = \kappa_r = \kappa$) and adopting the mean-field approximation,[34,35] quantum fluctuation terms are neglected such that $\langle a\rangle = \alpha$ represents the intracavity field amplitude. The steady-state solution for α is given by

$$\alpha = \frac{\sqrt{\kappa/\tau}(\alpha_{in,l} + \alpha_{in,r})}{\kappa - \mathrm{i}(\Delta_p - \Delta_{ac}) - \frac{2g^2N(r-\Gamma)(\Gamma+2\mathrm{i}\Delta_p)}{8g^2\Gamma|\alpha|^2 + (r+\Gamma)(\Gamma^2+4\Delta_p^2)}}. \tag{12}$$

The appearance of the intracavity intensity term $|\alpha|^2$ in the denominator indicates that the intracavity field can exhibit nonlinear dependence on the probe field under appropriate conditions.

The output fields are obtained from the standard input–output relations[36]

$$\alpha_{out,l} = \sqrt{\kappa\tau}\alpha - \alpha_{in,l}, \tag{13}$$

$$\alpha_{out,r} = \sqrt{\kappa\tau}\alpha - \alpha_{in,r}. \tag{14}$$

For simplicity, we define $\alpha_{in,r} = |\alpha_{in}|$ and $\alpha_{in,l} = |\alpha_{in}|e^{\mathrm{i}\phi}$, where ϕ is the relative phase between the probe fields. When CPA occurs, namely, $\alpha_{out,l} = \alpha_{out,r} = 0$, the relative phase satisfies $\phi = 0$, and the following condition holds:

$$\frac{2\kappa|\alpha_{in}|}{\kappa - \mathrm{i}(\Delta_p - \Delta_{ac}) - \frac{2g^2N(r-\Gamma)(\Gamma+2\mathrm{i}\Delta_p)}{8g^2\Gamma|\alpha|^2 + (r+\Gamma)(\Gamma^2+4\Delta_p^2)}} - |\alpha_{in}| = 0. \tag{15}$$

Solving this equation yields two conditions for CPA

$$\Delta_{ac} = \Delta_p\frac{\Gamma - 2\kappa}{\Gamma}, \tag{16}$$

$$|\alpha|^2 = \frac{N(\Gamma - r)}{4\kappa} - \frac{(\Gamma + r)(\Gamma^2 + 4\Delta_p^2)}{8g^2\Gamma}. \tag{17}$$

Compared with the proposal of Zhu *et al.*,[35] we further consider the influence of the incoherent field on the CPA criterion and show that perfect photon absorption can occur not only in the linear excitation regime but also in the nonlinear excitation regime of the cavity QED system. Perfect photon absorption is generally achievable under strong coupling conditions. In addition, our study focuses on optimizing the output-field characteristics and enhancing switching efficiency via the incoherent field. Consequently, multiple manipulation pathways can be realized through either the incoherent field or the relative phase. In the following section, we analyze the properties of tunable CPA, the input–output relations, and the corresponding all-optical switching behavior.

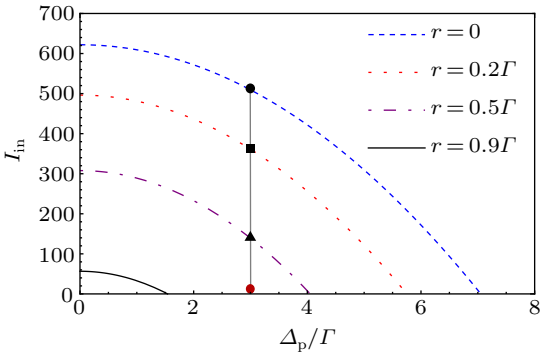


Fig. 2. Input intensity (arbitrary units) as a function of frequency under the CPA state. The blue dashed line, the red dotted line, the purple dot–dashed line, and the black solid line represent $r = 0$, $r = 0.2\Gamma$, $r = 0.5\Gamma$, and $r = 0.9\Gamma$, respectively. Other parameters are $\kappa = \Gamma$, $\tau = 0.01\kappa$, $g\sqrt{N} = 10\Gamma$, and $g = 0.02\Gamma$.

3. Analysis of numerical results

CPA occurs when the relative phase is $\phi = 0$ at which the probe fields interfere constructively on the surface of the lossy medium, resulting in the complete absorption of the probe fields with specific amplitude and frequency. Figure 2 illustrates the relation between the input intensity I_{in} and the frequency detuning Δ_p under CPA conditions. The results demonstrate that at identical detuning values, the required probe-field intensity for achieving CPA significantly decreases when incoherent pump field is applied. For example, at $\Delta_p = 3\Gamma$ (as indicated by the gray solid line in Fig. 2), when the pump rate $r = 0$, CPA condition is satisfied with

$I_{\rm in} \approx 510$ as shown by the black dot. Increasing the pump rate to $r = 0.2\Gamma$, the intensity of the probe field to achieve CPA decreases to $I_{\rm in} \approx 361$, as indicated by the black square. When the pump rate is further increased to $r = 0.5\Gamma$, CPA achieves at $I_{\rm in} \approx 137$, as shown by the black triangle. This demonstrates that increasing the pump rate can significantly lower the probe field intensity for realizing CPA, which provides a potential approach to weak-field nonlinear CPA. Additionally, increasing the pumping rate transfers more particles to the energy level $|2\rangle$, thereby reducing the absorption of the probe field. Consequently, the frequency threshold required for CPA decreases with the incoherent pumping rate.

When the pumping rate equals the decay rate of level $|2\rangle$, CPA cannot be achieved, and CPT is formed instead. Figure 3 shows the input–output relation of the cavity QED system under different pumping rates and relative phases. At $r = 0$, the CPA threshold is $\Delta_{\rm p} \approx 7\Gamma$ (see the blue dashed line in Fig. 2), which is consistent with previous studies, where CPA occurs in the linear regime at the threshold frequency.[37] When the frequency deviates from the threshold, for example, at $\Delta_{\rm p} = 6.5\Gamma$, CPA appears in a generally nonlinear regime with $I_{\rm in} \approx 95.2$, as shown by the blue solid line in Fig. 3(a). As $\Delta_{\rm p}$ decreases further, for example, to $\Delta_{\rm p} = 6\Gamma$, a higher input intensity is required to achieve CPA, which occurs in the bistable regime, as indicated by the green pattern in Fig. 3(c). However, the incoherent pump field reconfigures the CPA condition, with increasing pumping rates leading to enhanced output intensity. In particular, when $r = \Gamma$, CPT is achieved, as shown by the orange dotted lines in Figs. 3(a) and 3(c). Alternatively, CPT can be realized by setting the relative phase to $\phi = \pi$. Under this condition, the input fields interfere destructively at the surface of the medium, such that no light is coupled into the cavity. Consequently, perfect output is obtained, as shown in Figs. 3(b) and 3(d). These results establish the theoretical basis for realizing a CPA–CPT all-optical switch in a cavity QED system.

Figure 4 illustrates the output–input ratio as a function of input intensity under the relative phases corresponding to CPA and CPT. In the absence of the pump field, CPA occurs under the conditions of a relative phase $\phi = 0$ and a frequency detuning $\Delta_{\rm p}$ within the CPA threshold, whereas CPT appears at $\phi = \pi$, independent of the frequency and intensity of the probe field. As shown in Figs. 4(a) and 4(b), when the relative phase is $\phi = \pi$, the contrast ratio remains constant at 1, confirming that the output intensity equals the input intensity. A stable CPT state can therefore be achieved under this condition, as indicated by the red dashed lines in Figs. 4(a) and 4(b). When the relative phase is $\phi = 0$, the contrast ratio varies nonlinearly with input intensity and reaches zero at CPA, as illustrated by the red dots in Figs. 4(a) and 4(b).

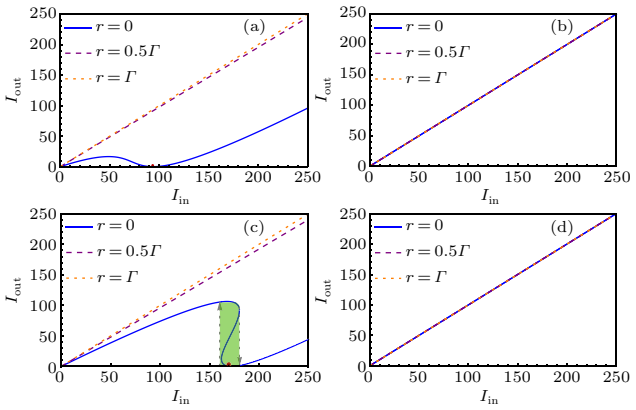


Fig. 3. Output intensity (arbitrary units) as a function of input intensity (arbitrary units) for (a) $\phi = 0$ and $\Delta_{\rm p} = 6.5\Gamma$, (b) $\phi = \pi$ and $\Delta_{\rm p} = 6.5\Gamma$, (c) $\phi = 0$ and $\Delta_{\rm p} = 6\Gamma$, and (d) $\phi = \pi$ and $\Delta_{\rm p} = 6\Gamma$. Other parameters are the same as those in Fig. 2.

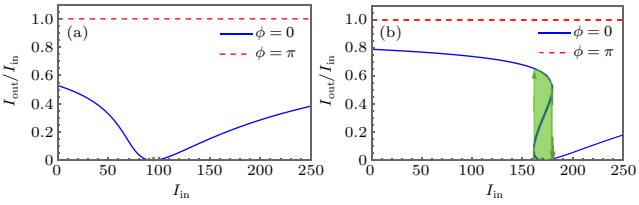


Fig. 4. Output–input ratio as a function of input intensity (arbitrary units) for (a) $\Delta_{\rm p} = 6.5\Gamma$ and (b) $\Delta_{\rm p} = 6\Gamma$ under the condition $r = 0$. Other parameters are the same as those in Fig. 2.

These results indicate that the all-optical switch is in the off state at the CPA point ($\phi = 0$) and in the on state at CPT ($\phi = \pi$). The switching efficiency is defined as

$$\eta = \frac{I_{\rm out}(\phi = \pi) - I_{\rm out}(\phi = 0)}{I_{\rm in}}. \tag{18}$$

Here, $I_{\rm out}(\phi = \pi)$ denotes the output intensity in the on state, which is equal to the input intensity, while $I_{\rm out}(\phi = 0)$ represents the output intensity in the off state and can be zero (CPA state) under appropriate conditions.[38]

Figure 5 shows the switching efficiency as a function of input intensity for different pumping rates. In the absence of incoherent pumping ($r = 0$), the switching efficiency exhibits distinct behaviors at different detunings. At $\Delta_{\rm p} = 6.5\Gamma$ (Fig. 5(a)), the efficiency increases nonlinearly with input intensity and reaches its maximum value at $I_{\rm in} \approx 95.2$ due to the occurrence of CPA, as indicated by the blue dashed curve. For $\Delta_{\rm p} = 6\Gamma$ (Fig. 5(b)), which is far from the CPA frequency threshold, the system exhibits bistable switching behavior. When the input intensity is increased to $I_{\rm in} \approx 179.2$, the efficiency jumps abruptly from $\eta \approx 0.52$ to $\eta \approx 0.98$. Conversely, when the input intensity is decreased to $I_{\rm in} \approx 161.8$, the efficiency drops nonlinearly from $\eta \approx 0.92$ to $\eta \approx 0.33$, as shown by the blue dashed curve. Notably, this bistability demonstrates phase-sensitive all-optical switching capability even in the absence of pumping.

With incoherent pumping ($r = 0.1\Gamma$), the maximum switching efficiency is achieved at lower input intensities

($I_{\rm in} \approx 65.4$ for $\Delta_{\rm p} = 6\Gamma$, red dotted curve in Fig. 5(b)), since CPA can be realized at reduced intensities with increasing pumping rate. At $r = 0.2\Gamma$, the detunings $\Delta_{\rm p} = 6.5\Gamma$ and $\Delta_{\rm p} = 6\Gamma$ lie outside the CPA frequency threshold, leading to a monotonic increase in output intensity at $\phi = 0$ with increasing input intensity and, consequently, a nonlinear reduction in the switching efficiency.

At $I_{\rm in} = 0$, a nonzero switching efficiency is observed, e.g., $\eta \approx 0.28$ for $\Delta_{\rm p} = 6.5\Gamma$ and $\eta \approx 0.80$ for $\Delta_{\rm p} = 6\Gamma$, which originates from the spontaneous emission of the excited level $|2\rangle$. When the pumping rate is increased to match the relaxation rate of level $|2\rangle$ (i.e., $r = \Gamma$), the output field enters the CPT state even at $\phi = 0$, and the switching efficiency remains zero, as indicated by the black solid curves in Fig. 5.

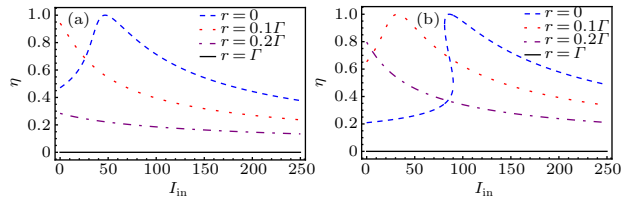


Fig. 5. Switching efficiency versus input intensity (arbitrary units), where (a) $\Delta_{\rm p} = 6.5\Gamma$ and (b) $\Delta_{\rm p} = 6\Gamma$. The blue dashed lines, red dotted lines, purple dash–dotted lines, and black solid lines represent $r = 0$, $r = 0.1\Gamma$, $r = 0.2\Gamma$, and $r = \Gamma$, respectively. Other parameters are the same as in Fig. 2.

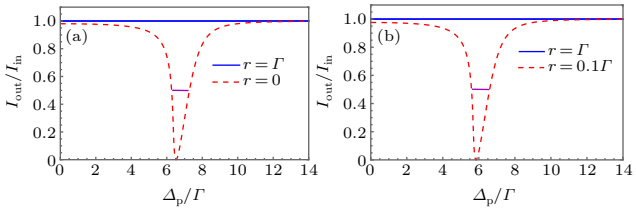


Fig. 6. Output–input ratio as a function of frequency detuning. The blue solid lines represent $r = \Gamma$, while the red dotted curves represent (a) $r = 0$ and (b) $r = 0.1\Gamma$. Other parameters are the same as in Fig. 2.

According to the study by Zhu *et al.*,[10] we consider two representative pumping rates: $r = 0$ and $r = 0.1\Gamma$. The frequency detuning of the probe field is defined as $\Delta_{\rm p} = \Delta \pm \delta$ under the two-photon resonance condition ($\Delta = \Delta_{\rm p}$), and the half-maximum intensity is given by $I(\Delta_{\rm p}) = (I_{\rm max} + I_{\rm min})/2$, where $I_{\rm max}$ is the output intensity when the switch is on, and $I_{\rm min}$ is the output intensity when the switch is off. As defined by Eq. (18), $I_{\rm max}$ corresponds to the pump field $r = \Gamma$, while $I_{\rm min}$ corresponds to $r = 0$ or $r = 0.1\Gamma$. The full width at half maximum (FWHM) is defined as $\delta = |\Delta_{\rm p1} - \Delta_{\rm p2}|$, yielding measured values of 6.025 MHz for $r = 0$ and 6.037 MHz for $r = 0.1\Gamma$ as shown in Fig. 6. The switching time, calculated as $t = 1/(2\pi\delta)$, is approximately $t \approx 0.026$ μs for both cases. These results indicate that the CPA-based all-optical switch achieves a rapid response time of ~ 26 ns.

Based on the above analysis, it is evident that a nonlinear optical switch can operate at maximum efficiency via CPA-CPT conversion. When an incoherent pump field is applied, the switch can achieve maximum efficiency with a weaker probe field, demonstrating that this scheme is suitable for high-efficiency switching even under relatively low signal conditions.

4. Conclusion

In summary, our investigation of a two-sided cavity QED system with an incoherent field has revealed several significant findings. We have demonstrated that nonlinear CPA or CPT can be realized under specific conditions. Notably, the transition between CPA and CPT states can be controlled by adjusting the phase relationship of the probe fields, transitioning from in-phase to out-of-phase configurations. The introduction of an incoherent field allows modulation of both the frequency range and input intensity required for the CPA state. A particularly interesting phenomenon occurs when the pumping rate matches the decay rate of the excited level, resulting in the conversion of the CPA state into a CPT state.

Based on these observations, we propose a controllable optical switch mechanism utilizing the CPA-CPT transition, which theoretically achieves maximum switching efficiency ($\eta = 1$) and can operate on the nanosecond timescale. Furthermore, our analysis reveals that the phase-dependent optical switch exhibits enhanced performance under weaker probe fields when a low-rate incoherent field is applied (e.g., $r = 0.1\Gamma$). The system also demonstrates potential as a bistable optical switch, showing high sensitivity to input intensity variations. These findings suggest promising applications in weak-signal detection and optical switching technologies. The proposed scheme provides a robust platform for controlling light–matter interactions and could contribute to the development of advanced photonic devices.

Acknowledgments

This project is supported by the National Natural Science Foundation of China (Grants Nos. 12304405, 12275203, and 12075176), the Natural Science Foundation of Shaanxi Provincial Department of Education (Grant No. 23JK0483), the Natural Science Basic Research Program of Shaanxi (Grant Nos. 2024JC-YBMS-521 and 2024JC-YBMS-039), the 2022 Shaanxi University Youth Innovation Team Project (Grant No. K20220186), and the College Students' Innovative Entrepreneurial Training Plan Program of Shaanxi (Grant No. S202410702178).

References

[1] Dawes A M, Illing L, Clark S M and Gauthier D J 2005 *Science* **308** 672
[2] Scheuer J, Sukhorukov A A and Kivshar Y S 2010 *Opt. Lett.* **35** 3712
[3] Bajcsy M, Hofferberth S, Balic V, Peyronel T, Hafezi M, Zibrov A S, Vuletic V and Lukin M D 2009 *Phys. Rev. Lett.* **102** 203902

[4] Kuno Y, Sakane S, Kasamatsu K, Ichinose I and Matsui T 2016 *Phys. Rev. A* **94** 063641
[5] Crenshaw M, Scalora M and Bowden C M 1992 *Phys. Rev. Lett.* **68** 911
[6] Scalora M and Bowden C M 1995 *Phys. Rev. A* **51** 4048
[7] Zhang X, Yi H, Yao Y, Wang S and Shi L 2023 *Chin. Phys. Lett.* **40** 124204
[8] Huang Y P, Altepeter J B and Kumar P 2010 *Phys. Rev. A* **82** 063826
[9] Rutckaia V and Schilling J 2020 *Nat. Photonics* **14** 4
[10] Wang L and Zhu Y 2022 *Opt. Lett.* **47** 830
[11] Li N, Xu J, Song G, Zhu C, Xie S, Yang Y, Zubairy M S and Zhu S Y 2016 *Phys. Rev. A* **93** 043819
[12] Chen F, Li H, Zhou H, Luo S, Sun Z, Ye Z, Sun F, Wang J, Zheng Y and Chen X 2022 *Phys. Rev. Lett.* **129** 057402
[13] Feng J, Wang J, Fieramosca A, Bao R, Zhao J, Su R, Peng Y, Liew T C, Sanvitto D and Xiong Q 2021 *Sci. Adv.* **7** eabj6627
[14] Wang S, Zhang X, Ma G and Zhu D 2023 *Chin. Phys. B* **32** 030506
[15] Chong Y D, Ge L, Cao H and Stone A D 2010 *Phys. Rev. Lett.* **105** 053901
[16] Wan W, Chong Y, Ge L, Noh H, Stone A D and Cao H 2011 *Science* **331** 889
[17] Longhi S 2010 *Phys. Rev. A* **82** 031801
[18] Novitsky D V 2019 *J. Opt.* **21** 085101
[19] Papaioannou M, Plum E, Valente J, Rogers E T and Zheludev N I 2016 *APL Photonics* **1** 090801
[20] Kang M, Zhang H, Zhang X, Yang Q, Zhang W and Han J 2018 *Phys. Rev. Appl.* **9** 054018
[21] Kakenov N, Balci O, Takan T, Ozkan V A, Altan H and Kocabas C 2016 *ACS Photonics* **3** 1531
[22] Jeffers J 2019 *Phys. Rev. Lett.* **123** 143602
[23] Suwunnarat S, Halpern D, Li H, Shapiro B and Kottos T 2019 *Phys. Rev. A* **99** 013834
[24] Del Hougne P, Yeo K B, Besnier P and Davy M 2021 *Laser Photon. Rev.* **15** 2000471
[25] Liu J C, Wang F L, Han J Y, Hao Y Z, Yang Y D, Xiao J L and Huang Y Z 2020 *J. Lightwave Technol.* **38** 1382
[26] Guo M D, Li H F, Wang F L, Zhou C X and Wu Y J 2023 *Opt. Lett.* **48** 4037
[27] Wong Z J, Xu Y L, Kim J, O'Brien K, Wang Y, Feng L and Zhang X 2016 *Nat. Photonics* **10** 796
[28] Reiserer A and Rempe G 2015 *Rev. Mod. Phys.* **87** 1379
[29] Wei Y H, Gu W J, Yang G, Zhu Y and Li G X 2018 *Phys. Rev. A* **97** 053825
[30] Suleymanzade A, Anferov A, Stone M, Naik R K, Oriani A, Simon J and Schuster D 2020 *Appl. Phys. Lett.* **116** 104001
[31] Dong B, Wan Y, Chow W W, Shang C, Prokoshin A, Alkhazraji E, Koscica R, Wang H and Bowers J E 2024 *Nat. Photonics* **18** 669
[32] Zetie K, Adams S and Tocknell R 2000 *Phys. Educ.* **35** 46
[33] Manzano D 2020 *AIP Adv.* **10** 025106
[34] Xiong W, Chen J, Fang B, Lam C H and You J 2020 *Phys. Rev. A* **101** 063822
[35] Agarwal G, Di K, Wang L and Zhu Y 2016 *Phys. Rev. A* **93** 063805
[36] Scully M O and Zubairy M S 1997 *Quantum Optics* (Cambridge: Cambridge University Press)
[37] Guo M D 2021 *Opt. Express* **29** 27653
[38] Guo M D, Wu Y J, Li N, Li H F and Zhou C X 2024 *Phys. Lett. A* **505** 129456